THE JOURNAL OF PHYSICAL CHEMISTRY C
A JOURNAL OF THE AMERICAN CHEMICAL SOCIETY

pubs.acs.org/JPCC

Article

Template Driven Self-Assembly of the Pentacene Structure on the Si(553)-Pb Surface

Paweł Nita,* Marek Dachniewicz, Mieczysław Jałochowski, Krisztián Palotás, and Mariusz Krawiec

Cite This: J. Phys. Chem. C 2022, 126, 17738−17745

Read Online

ACCESS | Metrics & More | Article Recommendations

ABSTRACT: The self-assembly of the pentacene molecules on the Pb-ordered Si(553) surface is studied with scanning tunneling microscopy and density functional theory methods. Within the surface coverage up to a single monolayer, pentacene was found to form two different chain-like structures. They vary in molecular density, but both exhibit long-range, one-dimensional ordering with longer molecular axes aligned along step edges. The low-density phase consists of single discontinuous molecular rows and adapts the template surface periodicity, while the high-density phase features triple molecular chains with the unit cell determined by the length of the pentacene molecules. Such an arrangement of the molecules is controlled by a subtle balance between molecule−molecule and molecule−substrate interactions.

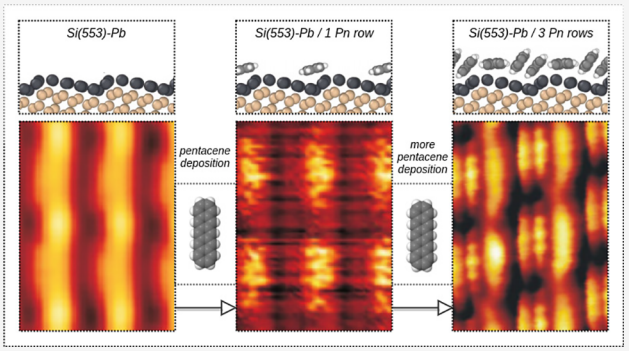

INTRODUCTION

Materials of π-conjugated organic molecules have been the subject of intensive research in recent years due to their great promise in electronic and optical devices applications, like organic transistors or solar cells.[1−3] Among these molecules, pentacene (Pn), $C_{22}H_{14}$, has attracted the interest of the scientific community due to its anisotropic charge transport and high carrier mobility without doping.[4]

From a technological point of view, molecular structures on the silicon surfaces are of particular interest, since they integrate their functionalities with the mainstream semiconductor electronics. However, self-assembly of molecules into regular patterns on bare silicon surfaces, e.g., Si(001)[5,6] or Si(111),[6,7] is impeded by a strong interaction of the molecules' π-electrons and the Si dangling bonds resulting in a disordered wetting layer.

To "deactivate" a silicon surface, passivation of the surface with a metal superstructure can be performed. The silicon (111) surface, modified by different metal atom species, was used as the template for pentacene molecule growth: Si(111)-$(\sqrt{3} \times \sqrt{3})$-Ag,[8,9] Si(111)-$(\sqrt{3} \times \sqrt{3})$-Au and Si(111)-$(5 \times 2)$-Au,[10] Si(111)-$\alpha(\sqrt{3} \times \sqrt{3})$-Bi[11] or Si(111)-$(\sqrt{7} \times \sqrt{3})$-In,[12] Si(111)-$\beta(\sqrt{3} \times \sqrt{3})$-Pb,[13] and Si(111)-$\sqrt{3} \times \sqrt{3}$-Ga.[13] However, the growth process on these surfaces is very diverse and not understood yet.

Pentacene is a planar molecule formed by five benzene rings, belonging to a class of polyacenes. Molecules in this group share the same bonding characteristics, i.e., σ bonds in the plane of the molecule and π bonds perpendicular to the plane of the molecule.

The arrangement of molecules is controlled by a subtle balance between molecule−molecule and molecule−substrate interactions. In many cases, the intermolecular forces, which determine the bulk structure of molecules, are very different from those acting on molecules adsorbed on a flat surface. Indeed, in the bulk phase, Pn has a layered herringbone structure,[14] while single layers of Pn can adsorb flat on strongly interacting surfaces or stand up as deposited on weakly interacting surfaces.[10,15−18] Usually, the deposition of Pn on flat surfaces results in multidomain formations, which is not very useful from a point of view of potential applications, although attempts with anisotropic surface reconstruction have also been made.[19,20]

To improve the ordering of Pn molecules, various vicinal (stepped) surfaces, mainly metallic, have been utilized. It is known that step edges act as nucleation centers for growing structures; thus, the presence of monatomic steps can improve the ordering of molecules, as it has been demonstrated many times for metallic vicinal surfaces.[21−31]

Received: July 27, 2022
Revised: September 23, 2022
Published: October 5, 2022

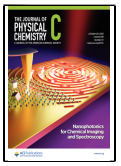

It is anticipated that directional and controlled growth of molecular nanostructures might also work on metal-stabilized vicinal silicon surfaces, like Si(*hhk*)-Au[32−34] and Si(*hhk*)-Pb.[35−38] Some of the substrates, prepatterned in such a way, have been proved as good templates to grow other metal atom species: Pb/Si(335)-Au,[39,40] In/Si(553)-Au,[41,42] Pb/Si(553)-Au,[43,44] Ag/Si(557)-Au,[45,46] or Sb/Si(553)-Pb.[47]

In this work, for the first time, we provide the experimental evidence of pentacene molecules self-assembled on metal-ordered vicinal Si surfaces. The pentacene structures have been epitaxially grown on the Si(553)-Pb substrate. The template morphology features five-atom-wide Pb nanoribbons that cover the Si substrate terraces completely, stabilizing the surface and deactivating Si dangling bonds. The deposition of Pn molecules results in two different chain-like structures, low- and high-density phases (LD and HD), as revealed by systematic scanning tunneling microscopy (STM) measurements. In both cases, the long axis of molecules is aligned parallel to the step edges, which indicates that the substrate triggers the long-range ordering of the pentacene structures. First-principles density functional theory (DFT) calculations point to the interplay between molecule−molecule and molecule−substrate interactions.

METHODS

Experimental Section. Experiments were carried out in an ultrahigh vacuum chamber with the base pressures lower than 10^{-10} mbar. The chamber was equipped with the VT STM (Omicron). The substrate was cut from the p-type, B-doped Si(553) wafer with specific resistivity 0.14 Ω·cm at RT. Once under vacuum, the sample was degassed for 12 h and flashed up to 1500 K in order to remove SiC crystallines. Subsequently, 1.3 ML of Pb (1 ML corresponds to the density of atoms in half of the bulk terminated Si(111) bilayer which is 7.84×10^{14} atoms/cm^2.) was deposited. A well-ordered surface was obtained by annealing the sample at 950 K for 5 min, and gradual temperature reduction was within the next 5 min. Pentacene (99.995%, Sigma) was deposited from a homemade, molybdenum crucible onto the sample kept at room temperature in a separate chamber. The sample was not annealed after pentacene deposition. The vertical distance between the evaporator and the sample was 15 cm. A quartz microbalance was used to control the deposition rate, that was chosen to be about 1 ML/4 min. In the following, we take one pentacene monolayer, the first, most densely packed layer of molecules adsorbed on the Si(553)-Pb surface. Such a quantity corresponds to a density of 12.4×10^{13} molecules/cm^2, as calculated from STM images. All STM measurements were performed with the sample maintained at 220 K in order to reduce Pn mobility. Tips were prepared from polycrystalline tungsten wire. Images were processed with WSxM[48] and Gwyddion.[49]

Calculations. The DFT calculations have been performed based on the projector augumented waves (PAWs)[50] and van der Waals corrected exchange-correlation functional (vdW-DF)[51] available in VASP (Vienna ab initio simulation package).[52,53] The optB86b-vdW implementation[54] of the vdW-DF method was used in all the calculations.

A kinetic energy cutoff of 300 eV for the plane wave expansion of single particle wave functions was used. The Brillouin zone was sampled by a 2 × 4 × 1 Monkhorst−Pack k-points grid.[55] The convergence for the total energy was chosen as 10^{-6} eV between subsequent iteration steps, and the maximum force allowed on each atom during the geometry optimization was less than 0.01 eV/Å. These parameters were tested and optimized to obtain well converged total energies of the system.

The Pb/Si(553) system, used as a substrate for pentacene adsorption, has been built according to the structural model of ref 37 and consists of four Si double layers and a single layer of Pb atoms on top of it. Si atoms of the bottom layer were saturated with hydrogen atoms and kept in their initial positions during relaxation processes. A single Pn molecule adsorbed on the Pb/Si(553) surface has been considered in a 7 × 1 supercell, i.e., $7a_{\mathrm{Si}[1\bar{1}0]} \times 1a_{\mathrm{Si}[331\bar{0}]}$, where $a_{\mathrm{Si}[1\bar{1}0]}$ and $a_{\mathrm{Si}[331\bar{0}]}$ are Si lattice constants along and across the step edges, respectively. A vacuum space of 14 Å was introduced to prevent any unphysical interaction between the periodic images of the slab. STM images were simulated assuming an s-type tip orbital (Tersoff-Hamann approximation) using the revised Chen method[56] implemented in the BSKAN code.[57,58]

RESULTS AND DISCUSSION

STM Topography. Figure 1 presents an STM topography image of the Si(553)-Pb surface. It consists of regularly

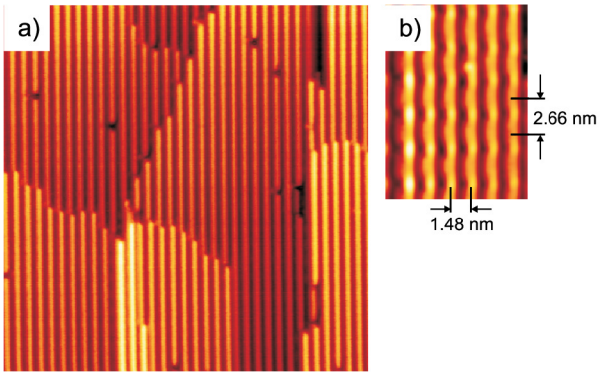

Figure 1. STM topography image of the Si(553)-Pb surface: a) 50 × 50 nm^2, $U = -1.8$ V, $I = 0.18$ nA and b) 10.4 × 14.2 nm^2, $U = +0.3$ V, $I = 1$ nA.

distributed steps and terraces separated by 1.48 nm in the $[11\bar{2}]$ direction. The deposited lead forms five-atom wide nanoribbons on each Si(111) terrace. The periodicity along the steps, i.e., in the $[1\bar{1}0]$ direction comes from the coincidence of 7 Si and 8 Pb unit cells and yields 2.69 nm. The structural model obtained by DFT calculations points to no mixing of Pb and Si atoms and to the weak coupling between both subsystems.[37] Furthermore, photoemission experiments and additional DFT calculations reveal a strong metallic and purely one-dimensional character of surface bands with strong spin−orbit interaction.[38]

Low-Density Phase. Figure 2 shows the STM topography image of the low-density phase of the pentacene. As calculated from the STM images, molecular density is 2.76×10^{13} mol/cm^2 (0.22 ML). Uniformly distributed discontinuous rows of fuzzy blobs are clearly visible. We identify these blobs as individual Pn molecules adsorbed with the long molecular axes oriented along the step edges of the template. In this case, the molecule−substrate interaction seems to be the main driving force of such an arrangement in the LD phase. However, Pn molecules are highly mobile making the STM measurements difficult at the experimental conditions. The main driving force

https://doi.org/10.1021/acs.jpcc.2c05308
J. Phys. Chem. C 2022, 126, 17738−17745

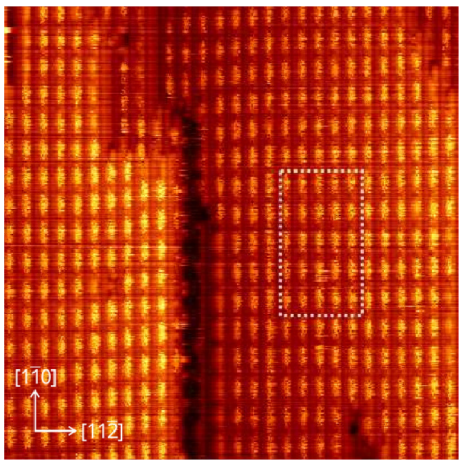

Figure 2. STM topography image (41 × 41 nm^2, 0.1 nA, −1.6 V) of the LD pentacene phase. The rectangle indicates the region selected for further analysis.

of the diffusion is the temperature, but the STM tip can also locally lower diffusion barriers.

Detailed topographic analysis of the LD phase is presented in Figure 3. The height profile measured across the steps shows

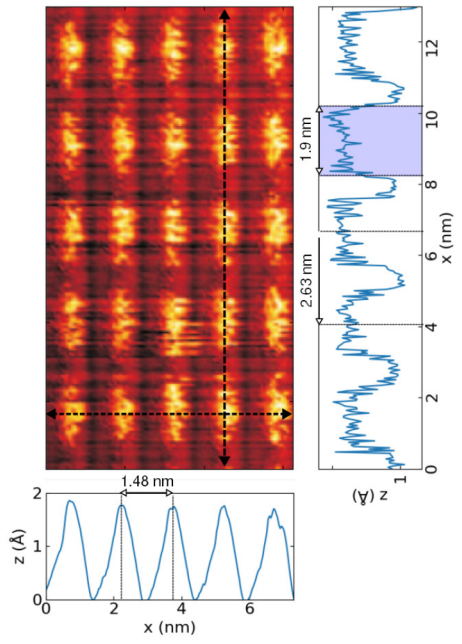

Figure 3. STM topography image and height profiles across steps (bottom panel) and along one step (right panel) in the LD phase.

the 1.48 nm wide terraces, confirming that the template is preserved upon Pn adsorption. Moreover, only single pronounced peaks in the profile indicate that there are only single molecules on terraces located close to the step edges.

The intermolecular distance measured along steps yields 2.63 nm (Figure 3) and reproduces the template periodicity. The average length of the molecules determined from the STM images is around 1.9 nm. Bearing in mind that the longer van der Waals radius of Pn is 1.56 nm, the observed objects appear to be longer. This discrepancy is associated with the diffusion of Pn molecules. Indeed, the fuzzy images together with the streak orientation and their specific behavior dependent on the scanning speed confirm this scenario.[43]

The fuzzy STM images of Pn molecules are caused most likely by three phenomena: (i) thermally driven diffusion, (ii) tip-activated motion along the steps, and (iii) the fluctuations of Pn orientation due to strong tip-molecules interaction. At the moment, it is unclear which mechanism dominates. The diffusion coefficients depend on the substrate crystallographic direction, and different molecular orientations were reported for Pn[25] or the "Violet Lander" molecule[59] on the Cu(110) surface. Mira et al.[60] showed that diffusion of azobenzene molecules along the [1$\bar{1}$0] direction is six times faster when their longer axis is parallel to the direction of motion than for molecules oriented perpendicular to the diffusion channel at low temperature. The STM tip induced motion of Pn molecules has been reported by Lagoute et al.[61] In the present case, the mismatch between the periodicity of acene rings and the Pb−Pb distance suppresses the corrugation of the potential energy surface and results in a privileged direction of motion of the molecules. However, the movement of the molecules along [1$\bar{1}$0] seems to be limited to the size of the surface unit cell. This would suggest the existence of energy barriers at the unit cell boundaries and stronger molecule−substrate than molecule−molecule interaction. At the end of this paragraph, it is worth mentioning that Pb diffusion from the sample to the tip also can be responsible for fuzzy images. The Pb atoms quite easily pass onto the STM tip and "drag" behind it while scanning. The tip shape and its electronic properties become unstable resulting in streaks on STM images.

High-Density Phase. Figure 4 shows a large area STM topography image of the high-density phase obtained after the

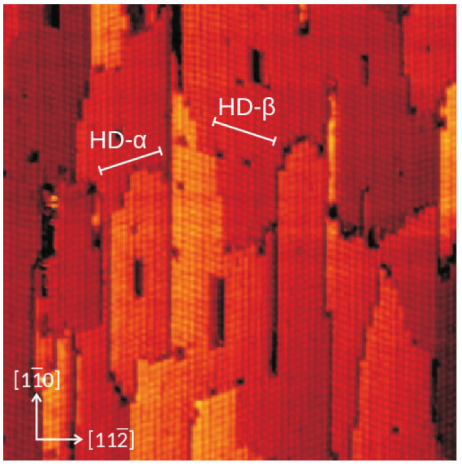

Figure 4. STM topography image of the HD phase recorded at sample bias U = −1.7 V and tunneling current I = 0.5 nA.

deposition of 1 ML of Pn. Two different configurations, HD-α and HD-β, appear. They form separate domains with the lateral size of tens of square nanometers.

Figure 5 shows a set of high-resolution STM images of the same area of the HD-α phase, recorded at different bias conditions. In the occupied states image, Figure 5a, we can distinguish three uniformly distributed molecular rows. Along the rows, molecules adopt head-to-head orientation, while across the steps, molecules form an ABC sequence. Note that molecules in rows B and C appear to be much narrower than molecules in row A, which suggests that their spatial

https://doi.org/10.1021/acs.jpcc.2c05308
J. Phys. Chem. C 2022, 126, 17738−17745

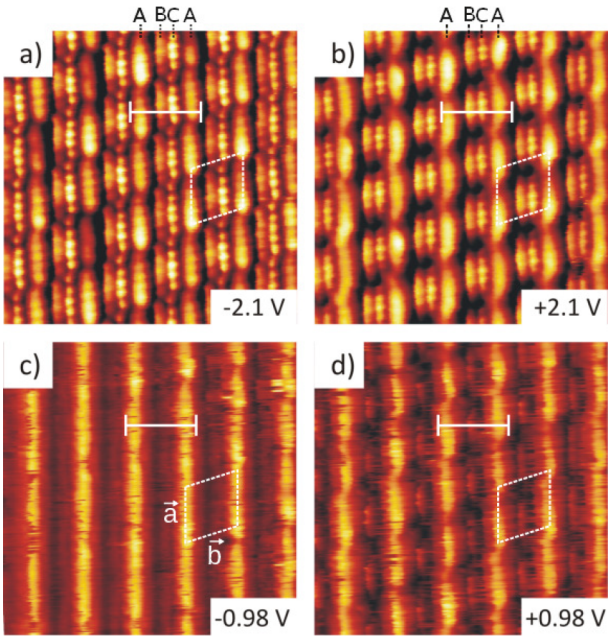

Figure 5. STM micrographs of the same area (10 × 10 nm^2, 0.4 nA): a) −2.1 V, b) +2.1 V, c) −0.98 V, and d) +0.98 V. Arrows and letters indicate rows of molecules within a single terrace. Dimensions of the unit cell are defined by vectors $\vec{a}$ = 1.62 nm and $\vec{b}$ = 1.56 nm, and the angle between them is γ = 70 deg.

orientation is different. All the molecules exhibit clear modulation of the STM topography. It is worthwhile to note that molecules belonging to adjacent rows are shifted with respect to each other along the [1 $\bar{1}$ 0] direction. In the empty states image, Figure 5b, the situation is analogous. Molecules in rows B and C are visible as narrow objects, while molecules in row A form featureless crescents. The possibility that any asymmetry in the observed objects is due to the STM tip was ruled out. The measurements were repeated several times on different samples and with different STM tips. Such substantial changes in appearance of individual molecules are supposed to be related to nonequivalent lateral positions within terraces as well as to their different spatial orientation.

Guaino et al.[62] showed that under certain STM recording conditions the Pn layer on Si(111)-($\sqrt{3} \times \sqrt{3}$)Ag can appear to be transparent, and the underneath substrate lattice can be resolved. A similar mechanism was found to work when imaging the HD-α phase with bias in the range between −1 V and +1 V. In the occupied states image recorded at −0.98 V (see Figure 5c), instead of three molecular rows (compared to the −2.1 V case), only one fuzzy chain on the terrace is resolved. This chain was assigned to the step edge of the template located underneath. On the other hand, in the empty states image (Figure 5d) recorded at +0.98 V, two types of chains appear: bright distinctly modulated chains and rows of faintly visible features between them. The first one is related to step edges of the Si(553)-Pb surface with some contribution from molecular states. The second one is related to the residual molecular states of molecules within row B or C. The mechanism of imaging of a molecular film or an underneath surface has already been reported and is well understood.[63,64] At higher STM bias voltages, the resonant tunneling through the energy levels of molecules dominates, while at lower bias, within the HOMO−LUMO gap, the tunneling occurs directly between the tip and the surface, thus allowing the substrate features to be resolved.

Figure 6 shows height profiles taken across the rows marked in Figure 5, which reveal additional information. The distance

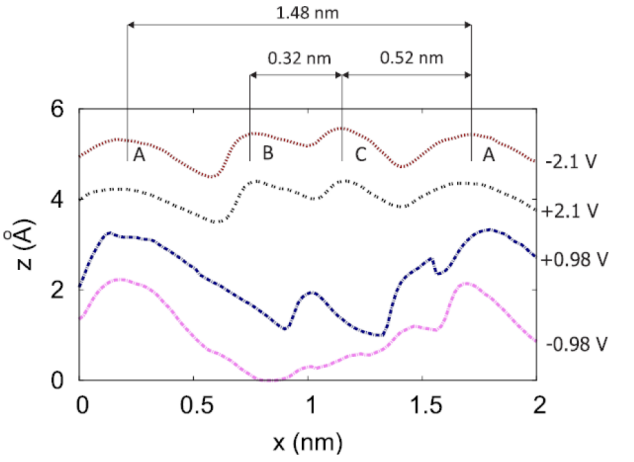

Figure 6. Height profiles measured across the steps (lines marked in Figure 5a, b, c, and d, respectively). Consecutive curves have been shifted for better visibility.

between consecutive A rows agrees with the terrace width of the template, namely 1.48 nm. The distance between adjacent B and C rows (within a single terrace) yields 0.32 nm, whereas the C−A distance is 0.52 nm. Considering the van der Waals size of an individual Pn molecule along the short axis is equal to 0.64 nm, it is clear that three Pn molecules cannot adsorb in the flat geometry within a single terrace, because there is not enough room for such an arrangement. Therefore, another structural configuration should be realized. Most likely molecules in rows B and C are rotated around their long axes; however, based solely on the STM topography measurements, it is impossible to determine the value and the direction of the rotation angle. Comparing the STM appearance of molecules in the A rows (see Figure 5a) with their lateral dimensions, the molecules lie flat on step edges or are only slightly tilted.

Height profiles taken along the rows are shown in Figure 7. Molecules in row C exhibit well resolved STM topography modulation consisting of five peaks separated by approximately 2.62 Å. This distance is slightly longer than the acene ring separation (2.45 Å) in the isolated Pn molecule. Moreover, molecules in adjacent rows B and C are shifted by 1.8 Å with respect to each other. This is almost 0.6 Å more than half of the acene ring separation (1.27 Å), and this may indicate that these molecules are stacked together due to the $\pi-\pi$ interaction. On the other hand, the displacement between molecules in consecutive A rows, i.e., on different Si(553) terraces, is around 5.0 Å (see Figure 7 a). This is commensurate with 1.5 × Pb nanoribbon lattice constant along the [1 $\bar{1}$ 0] direction, namely 4.9 Å. These facts seem to indicate that such a peculiar arrangement of the molecules is due to a delicate balance between molecule−molecule and molecule−substrate interactions. Both mechanisms must play a significant role, and one can expect that the higher the Pn density the stronger the molecule−molecule interaction.

It is worthwhile to note that the height profiles measured along the A rows show the enhanced density of the states at one end of the molecules. It may indicate that the molecules

https://doi.org/10.1021/acs.jpcc.2c05308
J. Phys. Chem. C 2022, 126, 17738−17745

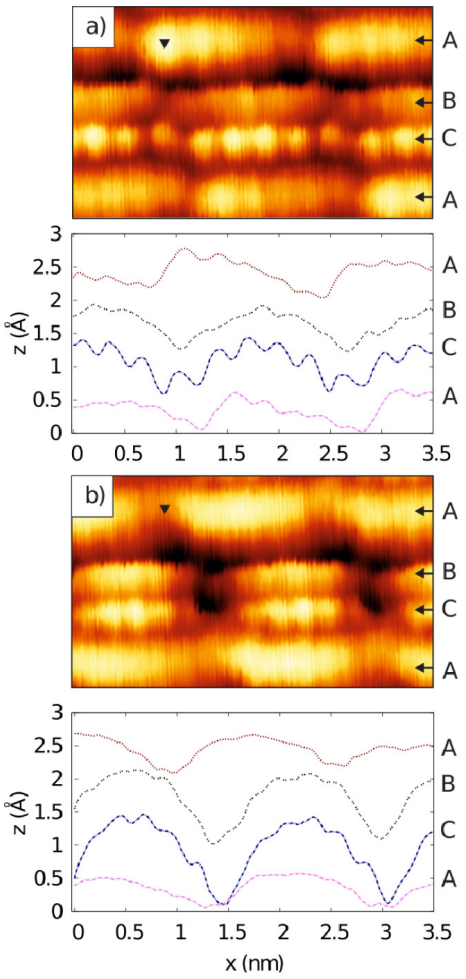

Figure 7. Height profiles measured along A, B, and C rows in occupied (a) and empty states images (b). Profiles have been shifted in order to avoid overlapping. Letters A, B, and C stand for the position of the corresponding molecular rows.

are tilted around its shorter axes with respect to the surface. The apparent height difference between their ends is around 0.5 Å which gives an angle value of 1.8 degrees. The plausible reason for the tilting can be explained by the incommensurate Pn molecule length (as well as the acene ring separation) and the atomic structure of Pb nanoribbons, which are not completely flat along the $[1\bar{1}0]$ direction. Note that the tilting in the α and β configurations is reversed. The tilting of the Pn molecules was observed in the "R" phase on Cu(111).[65] In the profiles measured in the empty states image (see Figure 7b), only the molecule in row C exhibits the clearly visible periodicity of 2.6 Å. The modulation in other rows (A or B) is not resolved at these tunneling parameters. Moreover, the molecules in the A rows do not show pronounced out of plane inclination, and the maximum intensity is detected in the middle of them.

Intermediate-Coverage Phase. It has been found in STM measurements of the surface covered by less than 1 ML Pn that only LD and HD phases exist. No other regular phase has been observed. Indeed, Figure 8 shows the STM topography of the boundary between the LD and HD phases. Evidently, the interface between both configurations is very sharp. Going from the top part of the image, we see single chains of the LD phase changing suddenly into the HD

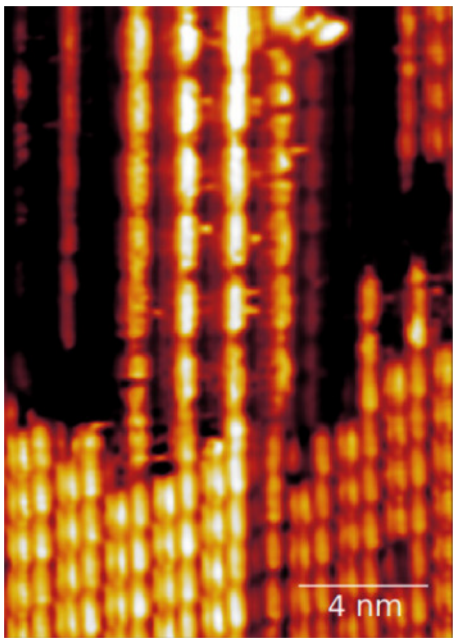

Figure 8. STM topography image ($U = -1.96$ V, $I = 0.26$ nA) of the Si(553)-Pb surface with intermediate pentacene coverage.

structure. There are very few two-molecule structures visible, which also confirms that the HD phase consists of three Pn molecules.

All these findings can help to elucidate the formation mechanism driven by the Pn coverage. At low coverage, Pn molecules occupy preferential adsorption sites on terraces of the Pb/Si(553). At this stage, the molecule−molecule interaction seems to be negligible; hence, the alignment along the step edges in a head-to-head configuration is dictated solely by template. When the coverage increases, molecules start to occupy other available sites on terraces. When the distance between adjacent molecules is comparable to their van der Waals dimensions, attractive forces start to play a significant role and lead to a lateral rearrangement in the row structure. Indeed, Steele[66] has shown that the lateral arrangement in films of linear molecules on graphite is strongly affected by the quadrupole interaction. Since Pn molecules exhibit relatively large quadrupole moments,[67] it is anticipated that this will substantially influence the Pn layout at the HD phase. A further increase in the pentacene dose results in the completion of the first layer in the form of a uniformly distributed row structure over macroscopic areas of the surface.

Geometry and Energetics. To address the structural properties of the pentacene decorated Pb/Si(553) surface, we have performed first-principles density functional theory calculations. Figure 9 shows relaxed atomic structures consistent with the experimentally found LD and HD phases.

In particular, the LD phase consists of a single Pn molecule in the Pb/Si(553) unit cell, while the HD phase has three Pn molecules per supercell. Pn molecules in the LD phase adsorb at step edges in a planar geometry. The HD phase is characterized by one Pn molecule horizontally oriented with respect to the surface and two vertically stacked molecules by $\pi-\pi$ bonding. Such arrangements of molecules are consistent with the experimental findings, which is also evident in simulated STM topography images shown in Figure 10.

The energetics of both systems are comparable to each other. The mean binding energy of a Pn molecule to the

https://doi.org/10.1021/acs.jpcc.2c05308
J. Phys. Chem. C 2022, 126, 17738−17745

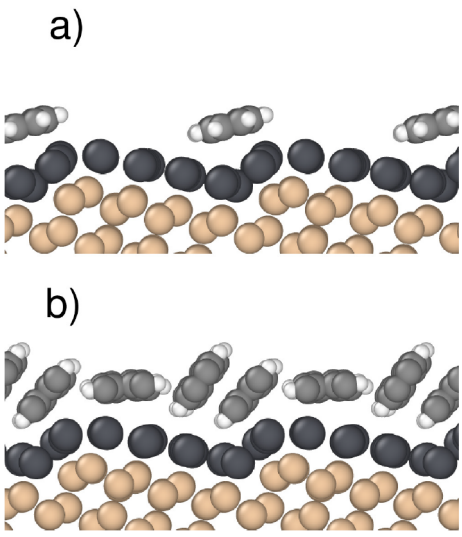

Figure 9. Structural model of pentacene on a Pb/Si(553) substrate obtained by DFT calculations: a) LD phase and b) HD phase. Silicon atoms are shown in light brown, Pb atoms are shown in dark gray, C atoms are shown in gray, and H atoms are shown in white.

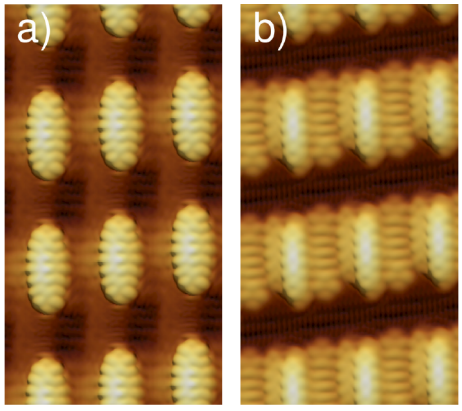

Figure 10. Simulated constant current filled states STM topography of the Si(553)-Pb/Pn surface, calculated for structural models shown in Figure 9.

substrate (E_b) is defined as the difference in total energy of the substrate with adsorbed molecules (E_{full}) and the sum of total energies of isolated Pn (E_{Pn}) molecules and the bare substrate (E_{surf})

$$E_b = (E_{full} - (NE_{Pn} + E_{surf}))/N \quad (1)$$

where N is the number of Pn molecules in the unit cell. Note that all of the above energies require fully relaxed geometries of the corresponding subsystems. The binding energy in the LD phase is equal to 2.19 eV, while the mean E_b in the HD phase yields 2.13 eV per molecule. According to the discussion above, it is expected that almost the full E_b in the LD phase goes to the molecule−substrate interaction, while in the HD phase, a substantial part of E_b is associated with the intermolecular interaction. To understand the energetics of the systems, it is convenient to introduce additional quantities: the interaction energy (E_{int}) and the deformation energies of Pn and the substrate (E^X_{def}, where $X \equiv Pn, surf$). The interaction energy is defined according to eq 1 but without additional geometry relaxation in the subsystems

$$E_{int} = (E_{full} - (NE^{froz}_{Pn} + E^{froz}_{surf}))/N \quad (2)$$

where E^{froz}_{Pn} and E^{froz}_{surf} are total energies of the Pn molecules and the substrate in frozen geometries taken from full slab calculations. The E_{int} calculated for the LD phase is equal to 2.30 eV. By comparing this energy to the E_b, one can conclude that only 0.11 eV goes to the deformation of the Pn molecule and the substrate and to the intermolecular interaction. The deformation energy (E^X_{def}) is defined as the total energy difference between corresponding subsystems with relaxed and frozen geometries:

$$E^X_{def} = E_X - E^{froz}_X \quad (3)$$

The E^{Pn}_{def} and E^{surf}_{def} in the LD phase are equal to 0.05 eV, which means that the geometries of both subsystems are almost unaffected by their mutual interaction. The remaining amount of energy can be assigned to the intermolecular interaction, which seems to be a reasonable value as Pn molecules are located in different unit cells. This means that the topography of the LD phase almost entirely is governed by the molecule−substrate interaction. Similar energy consideration for the HD phase leads to different conclusions. The mean interaction energy between a single Pn molecule and the substrate, E_{int}, yields 1.56 eV, which is 0.57 eV lower than the corresponding mean binding energy E_b. On the other hand, the deformation energy of the surface is E^{surf}_{def} = 0.03 eV per Pn molecule. This means that more than half of an electronvolt is responsible for the interaction between Pn molecules, which is approximately one-fourth of the total mean binding energy. Thus, the intermolecular interaction is an important factor in the formation of the HD layer and cannot be neglected.

The above energy considerations have been based on DFT calculations in the slab geometry with the surface unit cell. While in the case of the LD case, this should be correct, and the conclusions for the energetics of the HD phase may be somewhat biased by such a surface unit cell. Note that the STM topography of the HD phase reveals a different unit cell than the substrate one, see Figure 5. Unfortunately, such a unit cell is incommensurate with the Pb/Si(553) unit cell, and it is impossible to perform full slab DFT calculations. However, to investigate the role of the unit cell in the energetics of the HD phase, additional calculations for frozen unsupported (without substrate) Pn molecules in the HD phase unit cell have been performed. It turns out that the mean interaction energy between Pn molecules is further increased by 0.15 eV. Thus, it is clear that the HD density phase is governed not only by the molecule−substrate but also by substantial intermolecular interaction.

CONCLUSIONS

In summary, we have shown the feasibility of using the vicinal silicon surface with lead nanoribbons as a template for self-assembly of pentacene molecules into regular arrays of quasi-1D chain-like structures. Systematic STM investigations revealed the existence of two stable pentacene phases. At low coverage, the molecules are arranged into single rows and adapt the template surface periodicity, while at high coverage (1 ML), the molecules form triple molecular rows with the unit cell determined by the length of pentacene molecules. Two rows of molecules in the high-density phase are stacked by $\pi-\pi$ bonding, whereas the molecules at the step edges almost adsorb in the planar geometry. Such an arrangement of

https://doi.org/10.1021/acs.jpcc.2c05308
J. Phys. Chem. C 2022, 126, 17738−17745

molecules is controlled by a subtle balance between molecule−molecule and molecule−substrate interactions, as revealed by DFT calculations.

Although pentacene has been studied extensively in recent years on different type of substrates, the self-organization on the stepped silicon surface modified with metal atoms is an entirely new idea. Metal-induced chain structures on vicinal Si(*hhk*) surfaces appear as an interesting class of templates for molecular assembly. They provide a plethora of quasi one-dimensional systems with widely tunable physicochemical properties. It is expected that the combination of this specific type of templates with vast organic molecules functionalities will allow the fabrication of novel low-dimensional materials, which encourages further work on such systems.

AUTHOR INFORMATION

Corresponding Author

Paweł Nita − *Faculty of Physics, Astronomy and Applied Computer Science, Jagiellonian University, 30-348 Cracow, Poland;* orcid.org/0000-0002-2332-3289; Email: pawel.nita@uj.edu.pl

Authors

Marek Dachniewicz − *Institute of Physics, Maria Curie-Skłodowska University, 20-031 Lublin, Poland*

Mieczysław Jałochowski − *Institute of Physics, Maria Curie-Skłodowska University, 20-031 Lublin, Poland;* orcid.org/0000-0003-4004-7666

Krisztián Palotás − *Institute for Solid State Physics and Optics, Wigner Research Center for Physics, H-1121 Budapest, Hungary; ELKH-SZTE Reaction Kinetics and Surface Chemistry Research Group, University of Szeged, H-6720 Szeged, Hungary;* orcid.org/0000-0002-1914-2901

Mariusz Krawiec − *Institute of Physics, Maria Curie-Skłodowska University, 20-031 Lublin, Poland;* orcid.org/0000-0002-8752-4928

Complete contact information is available at: https://pubs.acs.org/10.1021/acs.jpcc.2c05308

Notes

The authors declare no competing financial interest.

ACKNOWLEDGMENTS

We acknowledge financial support from the Foundation for Polish Science under HOMING PLUS Project No. 2013-08/10. K. P. acknowledges financial support from the National Research Development and Innovation Office of Hungary under project No. FK124100 and the János Bolyai Research Scholarship of the Hungarian Academy of Sciences.

REFERENCES

(1) Klauk, H. Organic Thin-Film Transistors. *Chem. Soc. Rev.* **2010**, *39*, 2643−2666.

(2) Wang, C.; Dong, H.; Hu, W.; Liu, Y.; Zhu, D. Semiconducting π-Conjugated Systems in Field-Effect Transistors: A Material Odyssey of Organic Electronics. *Chem. Rev.* **2012**, *112*, 2208−2267.

(3) Facchetti, A. Semiconductors for Organic Transistors. *Mater. Today* **2007**, *10*, 28−37.

(4) Dimitrakopoulos, C. D.; Kymissis, I.; Purushothaman, S.; Neumayer, D. A.; Duncombe, P. R.; Laibowitz, R. B. Low-Voltage, High-Mobility Pentacene Transistors with Solution-Processed High Dielectric Constant Insulators. *Adv. Mater.* **1999**, *11*, 1372−1375.

(5) Meyer zu Heringdorf, F.-J.; Reuter, M. C.; Tromp, R. M. Growth Dynamics of Pentacene Thin Films. *Nature* **2001**, *412*, 517−520.

(6) Kury, P.; Roos, K. R.; Thien, D.; Möllenbeck, S.; Wall, D.; Horn-von Hoegen, M.; Meyer zu Heringdorf, F.-J. Disorder-Mediated Ordering by Self-Interfactant Effect in Organic Thin Film Growth of Pentacene on Silicon. *Org. Electron.* **2008**, *9*, 461−465.

(7) Al-Mahboob, A.; Sadowski, J. T.; Nishihara, T.; Fujikawa, Y.; Xue, Q. K.; Nakajima, K.; Sakurai, T. Epitaxial Structures of Self-Organized, Standing-up Pentacene Thin Films Studied by LEEM and STM. *Surf. Sci.* **2007**, *601*, 1304−1310.

(8) Guaino, Ph.; Carty, D.; Hughes, G.; Moriarty, P.; Cafolla, A. A. Scanning Tunneling Microscopy Study of Pentacene Adsorption on Ag/Si(111)-($\sqrt{3}\times\sqrt{3}$)R30°. *Appl. Surf. Sci.* **2003**, *212−213*, 537−541.

(9) Teng, J.; Guo, J.; Wu, K.; Wang, E. Temperature and Coverage Driven Condensation of Pentacene on the Si(111)-($\sqrt{3}\times\sqrt{3}$)R30°-Ag Surface. *J. Phys.: Condens. Matter* **2007**, *19*, 356005.

(10) Thayer, G. E.; Sadowski, J. T.; Meyer zu Heringdorf, F.-J.; Sakurai, T.; Tromp, R. M. Role of Surface Electronic Structure in Thin Film Molecular Ordering. *Phys. Rev. Lett.* **2005**, *95*, 256106.

(11) Shimada, T.; Ohtomo, M.; Suzuki, T.; Hasegawa, T.; Ueno, K.; Ikeda, S.; Saiki, K.; Sasaki, M.; Inaba, K. Step-Bunched Bi-Terminated Si(111) Surfaces as a Nanoscale Orientation Template for Quasisingle Crystalline Epitaxial Growth of Thin Film Phase Pentacene. *Appl. Phys. Lett.* **2008**, *93*, 223303.

(12) Suzuki, T.; Yagyu, K.; Tochihara, H. Initial Growth of Pentacene on Si(111)-$\sqrt{7}\times\sqrt{3}$-In Surface. *Phys. Chem. Chem. Phys.* **2020**, *22*, 14748−14755.

(13) Teng, J.; Guo, J.; Wu, K.; Wang, E. Structure Versus Electron ffects in The Growth Mode of Pentacene on Metal-Induced Si(111)-$\sqrt{3}\times\sqrt{3}$ Surfaces. *J. Chem. Phys.* **2008**, *129*, 034703.

(14) Söhnchen, S.; Lukas, S.; Witte, G. Epitaxial Growth of Pentacene Films on Cu(110). *J. Chem. Phys.* **2004**, *121*, 525.

(15) France, C. B.; Schroeder, P. G.; Forsythe, J. C.; Parkinson, B. A. Scanning Tunneling Microscopy Study of the Coverage-Dependent Structures of Pentacene on Au(111). *Langmuir* **2003**, *19*, 1274−1281.

(16) Satta, M.; Iacobucci, S.; Larciprete, R. Molecular Adsorption and Multilayer Growth of Pentacene on Cu(111): Layer Structure and Energetics. *Phys. Rev. B* **2007**, *75*, 155401.

(17) Chiodi, M.; Gavioli, L.; Beccari, M.; Di Castro, V.; Cossaro, A.; Floreano, L.; Morgante, A.; Kanjilal, A.; Mariani, C.; Betti, M. G. Interaction Strength and Molecular Orientation of a Single Layer of Pentacene in Organic-Metal Interface and Organic-Organic Heterostructure. *Phys. Rev. B* **2008**, *77*, 115321.

(18) Neff, J. L.; Götzen, J.; Li, E.; Marz, M.; Hoffmann-Vogel, R. Molecular-resolution imaging of pentacene on KCl(001). *Beilstein J. Nanotechnol.* **2012**, *3*, 186−191.

(19) Zhang, H.; Li, Y.; Li, B.; Fang, X.; Ji, H.; Wang, B.; Zeng, Ch.; Hou, J. G. Templated Growth of Quasi-One Dimensional Molecular Structures on Si(111)-(4×1)-In Surface. *Surf. Sci.* **2009**, *603*, L70−L73.

(20) Garlant, A.; Maughan, B.; Zahl, P.; Monti, O. L. H2Pc and Pentacene on Cu(110)-(2× 1)O: A Combined STM and nc-AFM Study. *Surf. Sci.* **2020**, *696*, 121590.

(21) Gavioli, L.; Fanetti, M.; Pasca, D.; Padovani, M.; Sancrotti, M.; Betti, M. G. Quasi-1D Pentacene Structures Assembled on the Vicinal Cu(119) Surface. *Surf. Sci.* **2004**, *566−568*, 624−627.

(22) Gavioli, L.; Fanetti, M.; Sancrotti, M.; Betti, M. G. Long-Range-Ordered Pentacene Chains Assembled on the Cu(119) Vicinal Surface. *Phys. Rev. B* **2005**, *72*, 035458.

(23) Baldacchini, C.; Mariani, C.; Betti, M. G. Adsorption of Pentacene on Filled d-Metal Surfaces: Long-Range Ordering and Adsorption Energy. *J. Chem. Phys.* **2006**, *124*, 154702.

(24) Fanetti, M.; Gavioli, L.; Sancrotti, M.; Betti, M. G. Morphology of Pentacene Films Deposited on Cu(119) Vicinal Surface. *Appl. Surf. Sci.* **2006**, *252*, 5568−5571.

(25) Müller, K.; Kara, A.; Kim, T. K.; Bertschinger, R.; Scheybal, A.; Osterwalder, J.; Jung, T. A. Multimorphism in Molecular Monolayers: Pentacene on Cu(110). *Phys. Rev. B* **2009**, *79*, 245421.

(26) Martínez-Blanco, J.; Ruiz-Osés, M.; Joco, V.; Sayago, D. I.; Segovia, P.; Michel, E. G. Ordered Structures of Pentacene on Cu(110). *J. Vac. Sci. Technol. B* **2009**, *27*, 863.
(27) Annese, E.; Vobornik, I.; Rossi, G.; Fujii, J. Pentacene Films on Cu(119). *Langmuir* **2010**, *26*, 19142−19147.
(28) Götzen, J.; Lukas, S.; Birkner, A.; Witte, G. Absence of Template Induced Ordering in Organic Multilayers: The Growth of Pentacene on a Cu(221) Vicinal Surface. *Surf. Sci.* **2011**, *605*, 577−581.
(29) Wang, Y. L.; Ji, W.; Shi, D. X.; Du, S. X.; Seidel, C.; Ma, Y. G.; Gao, H.-J.; Chi, L. F.; Fuchs, H. Structural Evolution of Pentacene on a Ag(110) Surface. *Phys. Rev. B* **2004**, *69*, 075408.
(30) Mete, E.; Domiroğlu, I.; Albayrak, E.; Ellialtioğlu, Ş.; Danişman, M. F. Influence of Steps on The Tilting and Adsorption Dynamics of Ordered Pentacene Films on Vicinal Ag(111) Surfaces. *J. Phys. Chem. C* **2012**, *116*, 19429−14933.
(31) Guaino, Ph.; Carty, D.; Hughes, G.; McDonald, O.; Cafolla, A. A. Long-range Order in a Multilayer Organic Film Templated by a Molecular-Induced Surface Reconstruction: Pentacene on Au(110). *Appl. Phys. Lett.* **2004**, *85*, 2777.
(32) Jałochowski, M.; Stróżak, M.; Zdyb, R. Gold-Induced Ordering on Vicinal Si(111). *Surf. Sci.* **1997**, *375*, 203.
(33) Zdyb, R.; Stróżak, M.; Jałochowski, M. Gold-Induced Faceting on Si(533) Surface Studied by RHEED. *Vacuum* **2001**, *63*, 107−112.
(34) Crain, J. N.; McChesney, J. L.; Zheng, F.; Gallagher, M. C.; Snijders, P. C.; Bissen, M.; Gundelach, C.; Erwin, S. C.; Himpsel, F. J. Chains of Gold Atoms With Tailored Electronic States. *Phys. Rev. B* **2004**, *69*, 125401.
(35) Tegenkamp, C.; Kallassy, Z.; Pfnür, H.; Günter, H.-L.; Zielasek, V.; Henzler, M. Switching Between One and Two Dimensions: Conductivity of Pb-Induced Chain Structures on Si(557). *Phys. Rev. Lett.* **2005**, *95*, 176804.
(36) Tegenkamp, C.; Lükermann, D.; Pfnür, H.; Slomski, B.; Landolt, G.; Dil, J. H. Fermi Nesting between Atomic Wires with Strong Spin-Orbit Coupling. *Phys. Rev. Lett.* **2012**, *109*, 266401.
(37) Kopciuszyński, M.; Dyniec, P.; Krawiec, M.; Łukasik, P.; Jałochowski, M.; Zdyb, R. Pb nanoribbons on the Si(553) surface. *Phys. Rev. B* **2013**, *88*, 155431.
(38) Kopciuszyński, M.; Krawiec, M.; Zdyb, R.; Jałochowski, M. Purely One-Dimensional Bands With a Giant spin-orbit splitting: Pb nanoribbons on Si(553) surface. *Sci. Rep.* **2017**, *7*, 46215.
(39) Kisiel, M.; Skrobas, K.; Zdyb, R.; Mazurek, P.; Jałochowski, M. Pb Chains on Ordered Si(335) Surface. *Phys. Lett. A* **2007**, *364*, 152−156.
(40) Krawiec, M. Pb Chains on Reconstructed Si(335) Surface. *Phys. Rev. B* **2009**, *79*, 155438.
(41) Ahn, J. R.; Kang, P. G.; Byun, J. H.; Yeom, H. W. Adsorbate-Induced Reconstruction of An Array of Atomic Wires: Indium on the Si(553)-Au Surface. *Phys. Rev. B* **2008**, *77*, 035401.
(42) Kang, P.-G.; Jeong, H.; Yeom, H. W. Microscopic Mechanism of Templated Self-Assembly: Indium Metallic Atomic Wires on Si(553)-Au. *Phys. Rev. B* **2009**, *79*, 113403.
(43) Nita, P.; Jałochowski, M.; Krawiec, M.; Stępniak, A. One-Dimensional Diffusion of Pb Atoms on the Si(553)-Au Surface. *Phys. Rev. Lett.* **2011**, *107*, 026101.
(44) Nita, P.; Zawadzki, G.; Krawiec, M.; Jałochowski, M. Structural and Electronic Properties of Double Pb Chains on the Si(553)-Au Surface. *Phys. Rev. B* **2011**, *84*, 085453.
(45) Krawiec, M.; Jałochowski, M. Array of Double Au-Ag Chains on the Si(557) Surface. *Appl. Surf. Sci.* **2010**, *256*, 4813−4817.
(46) Krawiec, M.; Jałochowski, M. Doping of The Step-Edge Si Chain: Ag on a Si(557)-Au Surface. *Phys. Rev. B* **2010**, *82*, 195443.
(47) Dachniewicz, M.; Kopciuszyński, M.; Żurawek, L.; Stróżak, M.; Krawiec, M.; Jałochowski, M. Evidence for Electronically Isolated Atomic Chains: Sb-Pb Structures on the Si(553) Surface. *J. Phys. Chem. C* **2021**, *125*, 15061−15068.
(48) Horcas, I.; Fernández, R.; Gómez-Rodríguez, J. M.; Colchero, J.; Gómez-Herrero, J.; Baro, A. M. WSXM: A Software For Scanning Probe Microscopy And a Tool For Nanotechnology. *Rev. Sci. Instrum.* **2007**, *78*, 013705.
(49) Nećas, D.; Klapetek, P. Gwyddion: An Open-Source Software For SPM Data Analysis. *Centr. Eur. J. Phys.* **2012**, *10*, 181−188.
(50) Blöchl, P. E. Projector Augumented-Wave Method. *Phys. Rev. B* **1994**, *50*, 17953.
(51) Dion, M.; Rydberg, H.; Schröder, E.; Langreth, D. C.; Lundqvist, B. I. Van der Waals Density Functional For General Geometries. *Phys. Rev. Lett.* **2004**, *92*, 246401.
(52) Kresse, G.; Furthmüller, J. Efficient Iterative Schemes For Ab Initio Total-Energy Calculations Using a Plane-Wave Basis Set. *Phys. Rev. B* **1996**, *54*, 11169.
(53) Kresse, G.; Joubert, D. From Ultrasoft Pseudopotentials to the Projector Augumented-Wave Method. *Phys. Rev. B* **1999**, *59*, 1758.
(54) Klimeš, J.; Bowler, D. R.; Michaelides, A. Van der Waals Density Functionals Applied to Solids. *Phys. Rev. B* **2011**, *83*, 195131.
(55) Monkhorst, H. J.; Pack, J. D. Special Points For Brillouin-Zone Integrations. *Phys. Rev. B* **1976**, *13*, 5188.
(56) Mándi, G.; Palotás, K. Chen's Derivative Rule Revisited: Role of Tip-Orbital Interference in STM. *Phys. Rev. B* **2015**, *91*, 165406.
(57) Hofer, W. A. Challenges and Errors: Interpreting High Resolution Images in Scanning Tunneling Microscopy. *Prog. Surf. Sci.* **2003**, *71*, 147−183.
(58) Palotás, K.; Hofer, W. A. Multiple Scattering in a Vacuum Barrier Obtained From Real-Space Wavefunctions. *J. Phys.: Condens. Matter* **2005**, *17*, 2705−2713.
(59) Otero, R.; Hümmelink, F.; Sato, F.; Legoas, S. B.; Thostrup, P.; Lægsgaard, E.; Stensgaard, I.; Galvão, D. S.; Besenbacher, F. Lock-and-Key Effect in The Surface Diffusion of Large Organic Molecules Probed by STM. *Nat. Mater.* **2004**, *3*, 779−782.
(60) Miwa, J. A.; Weigelt, S.; Gersen, H.; Besenbacher, F.; Rosei, F.; Linderoth, T. R. Azobenzene on Cu(110): Adsorption Site-Dependent Diffusion. *J. Am. Chem. Soc.* **2006**, *128*, 3164−3165.
(61) Lagoute, J.; Kanisawa, K.; Fölsch, S. Manipulation and Adsorption-Site Mapping of Single Pentacene Molecules on Cu(111). *Phys. Rev. B* **2004**, *70*, 245415.
(62) Guaino, Ph.; Cafolla, A. A.; Carty, D.; Sheerin, G.; Hughes, G. An STM Investigation of the Interaction and Ordering of Pentacene Molecules on the Ag/Si(111)-($\sqrt{3}\times\sqrt{3}$)R30° Surface. *Surf. Sci.* **2003**, *540*, 107−116.
(63) Kanai, M.; Kawai, T.; Motai, K.; Wang, X. D.; Hashizume, T.; Sakura, T. Scanning Tunneling Microscopy Observation of Copper-Phthalocyanine Molecules on Si(100) and Si(111) Surfaces. *Surf. Sci.* **1995**, *329*, L619.
(64) Upward, M. D.; Beton, P. H.; Moriarty, P. Adsorption of Cobalt Phthalocyanine on Ag Terminated Si(111). *Surf. Sci.* **1999**, *441*, 21−25.
(65) Smerdon, J. A.; Bode, M.; Guisinger, N. P.; Guest, J. R. Monolayer and Bilayer Pentacene on Cu(111). *Phys. Rev. B* **2011**, *84*, 165436.
(66) Steele, W. Monolayers of Linear Molecules Adsorbed on the Graphite Basal Plane: Structures and Intermolecular Interactions. *Langmuir* **1996**, *12*, 145−153.
(67) Silinish, E. A.; Capek, V.*Organic Molecular Crystals: Interaction, Localization, and Transport Phenomena*. American Institute of Physics Press: New York, 1994.

https://doi.org/10.1021/acs.jpcc.2c05308
J. Phys. Chem. C 2022, 126, 17738−17745